

Relativistic Kadanoff-Baym equations for correlated initial states and baryogenesis

Mathias Garny (TU München)

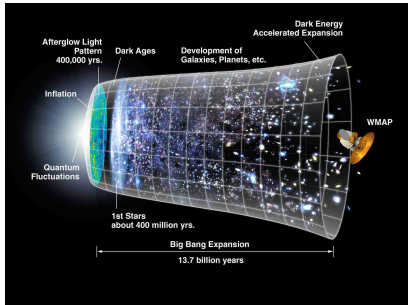
KBE2010, CAU Kiel, 23–26.03.2010

based on Phys.Rev.D80:085011,2009 with Markus Michael Müller
ongoing work with Urko Reinosa

Relativistic Kadanoff-Baym equations for correlated initial states and baryogenesis

- Motivation: Baryogenesis
- Relativistic Kadanoff-Baym Equations
- UV divergences, renormalization and Non-Gaussian ICs
- Results for $\lambda\Phi^4$ 2PI 3-loop
- Numerical methods

Nonequilibrium dynamics at high energy

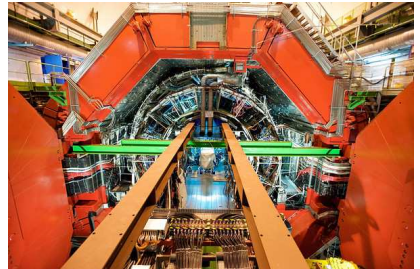


Heavy Ion Collisions

- LHC: ALICE
- RHIC

Early universe

- Reheating after Inflation
- Baryogenesis
- ...

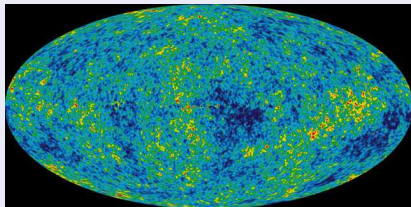


Baryon asymmetry of the universe

- Our galaxy consists of matter: $\bar{p}/p \lesssim 10^{-3}$
- No annihilations observed

Asymmetry parameter

$$\eta = \frac{n_b - n_{\bar{b}}}{s}$$



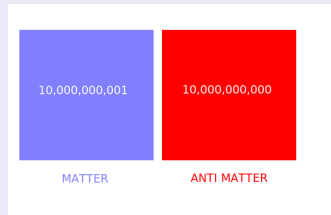
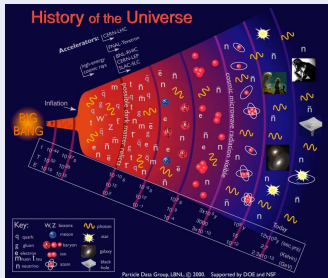
n_b = baryon density

$n_{\bar{b}}$ = anti-baryon density

s = entropy density

$$4.7 \cdot 10^{-10} < \eta < 6.5 \cdot 10^{-10} \text{ (95\% CL)}$$

Baryon asymmetry of the universe

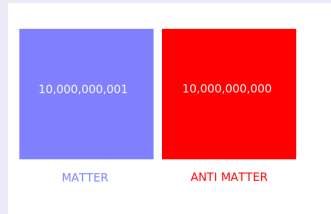
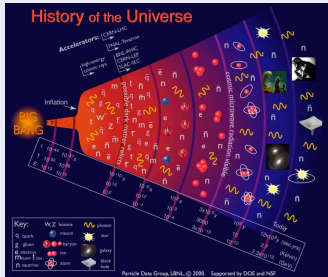


(1) Initial baryon asymmetry after Big Bang

Problem:

- Diluted by inflation
- Washed out by $\Delta B \neq 0$ processes at high energy

Baryon asymmetry of the universe



(1) Initial baryon asymmetry after Big Bang

Problem:

- Diluted by inflation
- Washed out by $\Delta B \neq 0$ processes at high energy

(2) Dynamical creation: **Baryogenesis**

Baryogenesis: three Sakharov conditions

Sakharov 1967

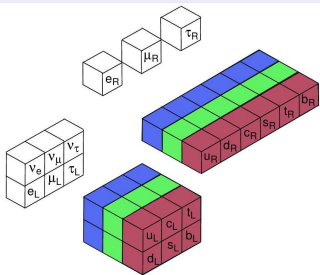
- baryon number violation: $\langle B \rangle \neq \text{const.}$
- CP violation: $\Gamma(i \rightarrow f) \neq \Gamma(\bar{i} \rightarrow \bar{f})$
- **deviation from thermal equilibrium**: $\Gamma(i \rightarrow f) \neq \Gamma(f \rightarrow i)$

Baryogenesis: three Sakharov conditions

Sakharov 1967

- baryon number violation: $\langle B \rangle \neq \text{const.}$
- CP violation: $\Gamma(i \rightarrow f) \neq \Gamma(\bar{i} \rightarrow \bar{f})$
- **deviation from thermal equilibrium**: $\Gamma(i \rightarrow f) \neq \Gamma(f \rightarrow i)$

Baryogenesis within the Standard Model of Particles ?



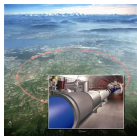
- B-violation for $T > T_{EW}$

$$\Delta B = \Delta L$$

- CP-violation in quark mixing
→ K^0/\bar{K}^0 decay
- Expanding universe

But: much too weak...

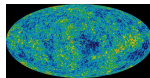
Baryogenesis



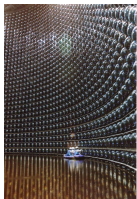
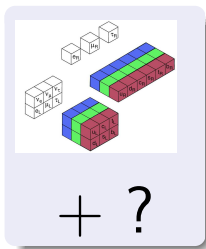
Collider exp.



Baryogenesis



$$4.7 \cdot 10^{-10} < \eta < 6.5 \cdot 10^{-10}$$



Neutrino
exp.



Dark matter



$$\frac{\rho_{\text{dark matter}}}{\rho_0} \simeq 0.23$$

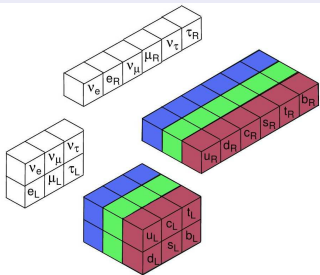
Superkamiokande
Neutrino Detector

Baryogenesis

Baryogenesis: three Sakharov conditions

- baryon number violation: $\langle B \rangle \neq \text{const.}$
- CP violation: $\Gamma(i \rightarrow f) \neq \Gamma(\bar{i} \rightarrow \bar{f})$
- **deviation from thermal equilibrium**: $\Gamma(i \rightarrow f) \neq \Gamma(f \rightarrow i)$

Baryogenesis in the SM + Right-handed neutrinos $(\nu_R)_{e,\mu,\tau}$



- B- via L-violation $M_R \bar{\nu}_R \nu_R^c$
 $\rightarrow 0\nu\beta\beta: (A, Z) \rightarrow (A, Z + 2) + 2e^-$
(Gerda, Nemo, Exo, ...)
- CP-violation in ν -mixing
 $\rightarrow \nu$ -oscillation
(Double Chooz, Daya Bay, ...)
- Expanding universe

Leptogenesis

Out-of-equilibrium decay of heavy right-handed neutrino ν_R

$$\mathcal{M}_{\nu_R, i \rightarrow \ell_{L, \alpha} h^\dagger} = \text{tree} + \text{loop} + \dots$$

$$\mathcal{M}_{\nu_R, i \rightarrow \ell_{L, \alpha}^c h} = \text{tree} + \text{loop} + \dots$$

CP violation in decay described by **loop process**

$$\Gamma(\nu_{R, i} \rightarrow \ell_{L, \alpha} h^\dagger) - \Gamma(\nu_{R, i} \rightarrow \ell_{L, \alpha}^c h) \sim \text{Im}(y_{i\alpha} y_{i\beta} y_{j\alpha}^* y_{j\beta}^*) \cdot \text{Im} \left(\text{loop diagram} \right)$$

Baryogenesis via Leptogenesis

- CP violation in decay described by **loop process**
- **deviation from thermal equilibrium**

Quantum nonequilibrium effects ?

Boltzmann equation for leptogenesis

$$\begin{aligned} p^\alpha \mathcal{D}_\alpha f_{\ell_L}(t, \mathbf{x}, \mathbf{p}) &= \int d\Pi_{\nu_R} d\Pi_h \\ &\times (2\pi)^4 \delta(p_{\ell_L} + p_h - p_{\nu_R}) \\ &\times \left[|\mathcal{M}|_{\nu_R \rightarrow \ell_L h^\dagger}^2 f_{\nu_R} (1 - f_{\ell_L}) (1 + f_h) \right. \\ &\quad \left. - |\mathcal{M}|_{\ell_L h^\dagger \rightarrow \nu_R}^2 f_{\ell_L} f_h (1 - f_{\nu_R}) \right] \end{aligned}$$



$|\mathcal{M}|^2$: microscopic interactions, **off-shell** processes

$f(t, \mathbf{x}, \mathbf{p})$: macroscopic propagation of **on-shell** particles

$$\Delta x_{interaction} \ll \lambda_{mfp}, \quad \lambda_{de-Broglie} \ll \lambda_{mfp}$$

$$1/M \ll 1/\Gamma, \quad 1/T \ll 1/(y^2 T)$$

Corrections within Boltzmann picture

Bose-enhancement, Pauli-Blocking; kinetic (non-)equilibrium

- quantum statistical factors $1 \pm f_k$
- non-integrated Boltzmann equations

Hannestad, Basbøll 06; Garayoa, Pastor, Pinto, Rius, Vives 09; Hahn-Woernle, Plümacher, Wong 09

Medium corrections

- medium correction to decay rates



$$\epsilon = \frac{\Gamma(\nu_R \rightarrow \ell h^\dagger) - \Gamma(\nu_R \rightarrow \ell^c h)}{\Gamma(\nu_R \rightarrow \ell h^\dagger) + \Gamma(\nu_R \rightarrow \ell^c h)} = \epsilon^{\text{vac}} + \delta\epsilon^{\text{th}}(T, \dots)$$

- thermal masses

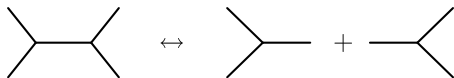
MG, Hohenegger, Kartavtsev, Lindner 09; Kiessig, Plümacher 09; Giudice, Notari, Raidal, Riotto, Stumia 04; Covi, Rius, Roulet, Vissani 98; . . .

Flavour effects

Nardi, Nir, Roulet, Racker 06; Adaba, Davidson, Ibarra, Josse-Micheaux, Losada, Riotto 06; Blanchet, diBari 06. . .

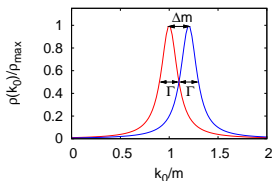
Limitations of the Boltzmann approach

- Unstable particles lead to double counting problems
[real intermediate state subtraction]



- Resonant Leptogenesis: $\Gamma \sim \Delta M$

Pilaftsis, Underwood, ...



- Quantum interference out of equilibrium

$$\epsilon = \frac{\Gamma(\nu_R \rightarrow \ell h^\dagger) - \Gamma(\nu_R \rightarrow \ell^c h)}{\Gamma(\nu_R \rightarrow \ell h^\dagger) + \Gamma(\nu_R \rightarrow \ell^c h)} \sim \text{diagram} \times \left(\text{diagram} \right)^* \sim 10^{-7}$$

Going beyond the Boltzmann picture

Statistical propagator $G_F^{ij}(x, y) = \langle \Phi^i(x)\Phi^j(y) + \Phi^j(y)\Phi^i(x) \rangle / 2$

Spectral function $G_\rho^{ij}(x, y) = i\langle \Phi^i(x)\Phi^j(y) - \Phi^j(y)\Phi^i(x) \rangle$

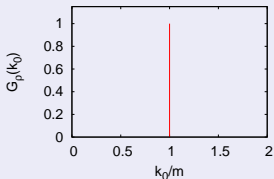
Going beyond the Boltzmann picture

Statistical propagator $G_F^{ij}(x, y) = \langle \Phi^i(x)\Phi^j(y) + \Phi^j(y)\Phi^i(x) \rangle / 2$

Spectral function $G_\rho^{ij}(x, y) = i \langle \Phi^i(x)\Phi^j(y) - \Phi^j(y)\Phi^i(x) \rangle$

Boltzmann limit

- on-shell quasi-stable particles



$$G_\rho^{ij}(k) \sim \delta^{ij} \delta(k^2 - m_i^2)$$

- equilibrium-like fluctuation-dissipation relation

$$G_F^{ij}(t, k) = \left(f_k^i(t) + \frac{1}{2} \right) G_\rho^{ij}(k)$$

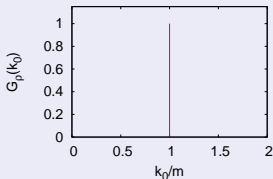
Going beyond the Boltzmann picture

Statistical propagator $G_F^{ij}(x, y) = \langle \Phi^i(x)\Phi^j(y) + \Phi^j(y)\Phi^i(x) \rangle / 2$

Spectral function $G_\rho^{ij}(x, y) = i \langle \Phi^i(x)\Phi^j(y) - \Phi^j(y)\Phi^i(x) \rangle$

Boltzmann limit

- on-shell quasi-stable particles



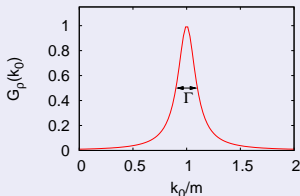
$$G_\rho^{ij}(k) \sim \delta^{ij} \delta(k^2 - m_i^2)$$

- equilibrium-like fluctuation-dissipation relation

$$G_F^{ij}(t, k) = \left(f_k^i(t) + \frac{1}{2} \right) G_\rho^{ij}(k)$$

Propagation beyond Boltzmann

- spectrum with (thermal) width



$$G_\rho^{ij}(t, k) \sim \frac{\delta^{ij} 2k_0 \Gamma_i(t)}{(k^2 - m_{th,i}^2(t))^2 + k_0^2 \Gamma_i(t)^2} + \dots$$

- on-/off-shell, cross-correlations

$$G_F^{ij}(t, k) = \begin{pmatrix} G_F^{11} & G_F^{12} \\ G_F^{21} & G_F^{22} \end{pmatrix}$$

Relativistic Kadanoff-Baym equations

$$\begin{aligned} (\partial_{x^0}^2 - \nabla_x^2 + m_i^2(x)) G_F^{ij}(x, y) &= \int_0^{y^0} d^4 z \Pi_F^{ik}(x, z) G_\rho^{kj}(z, y) \\ &\quad - \int_0^{x^0} d^4 z \Pi_\rho^{ik}(x, z) G_F^{kj}(z, y) \end{aligned}$$

$$(\partial_{x^0}^2 - \nabla_x^2 + m_i^2(x)) G_\rho^{ij}(x, y) = \int_{x_0}^{y^0} d^4 z \Pi_\rho^{ik}(x, z) G_\rho^{kj}(z, y)$$

Statistical propagator $G_F^{ij}(x, y) = \langle \Phi^i(x) \Phi^j(y) + \Phi^j(y) \Phi^i(x) \rangle / 2$

Spectral function $G_\rho^{ij}(x, y) = i \langle \Phi^i(x) \Phi^j(y) - \Phi^j(y) \Phi^i(x) \rangle$

Relativistic Kadanoff-Baym equations

Obtained from stationarity condition of the 2PI effective action

Cornwall, Jackiw, Tomboulis (1974)

$$\frac{\delta\Gamma[\phi, G]}{\delta G} = 0 \quad \Leftrightarrow \quad G^{-1} = G_0^{-1} - \Pi[G]$$

where $G(x, y) = G_F(x, y) - i/2 \text{sign}_{\mathcal{C}}(x^0 - y^0) G_\rho(x, y)$

Controlled approximation...

... by truncation of the 2PI functional $\Gamma_2[\phi, G]$

Relativistic Kadanoff-Baym equations

Example: Three-loop truncation in $\lambda\phi^4$ -theory (for $\langle\phi\rangle = 0$)

$$\Gamma_2[G] = \text{diagram 1} + \text{diagram 2}$$

The first diagram is a figure-eight loop with two external vertices. The second diagram is a circle with two internal lines forming a loop, and two external vertices.

$$\Pi[G] = \frac{2i\delta\Gamma_2}{\delta G} = \text{diagram 3} + \text{diagram 4}$$

The third diagram is a tadpole loop on a horizontal line with two external vertices. The fourth diagram is a circle with two external vertices.

$$S = \int d^4x \left(\frac{1}{2} \partial_\mu \phi \partial^\mu \phi - \frac{1}{2} m^2 \phi^2 - \frac{\lambda}{4!} \phi^4 \right)$$

$$\text{diagram 5} = -i\lambda \delta(x_1 - x_2) \delta(x_1 - x_3) \delta(x_1 - x_3)$$

The diagram is a four-point vertex represented by a central black dot with four lines extending outwards.

$$\text{diagram 6} = G(x, y)$$

The diagram is a horizontal line with two black dots at its ends.

Relativistic Kadanoff-Baym equations

Setting-sun approximation for $\lambda\Phi^4$ -theory

$$\begin{aligned}
 \left(\square_x + m^2 + \text{self-energy} \right) G_F(x, y) &= \int_0^{y^0} d^4z \left(\text{red circle} + \text{green circle} \right) G_\rho(z, y) \\
 &\quad - \int_0^{x^0} d^4z \left(\text{red circle} + \text{green circle} \right) G_F(z, y) \\
 \left(\square_x + m^2 + \text{self-energy} \right) G_\rho(x, y) &= \int_{x_0}^{y^0} d^4z \left(\text{red circle} + \text{green circle} \right) G_\rho(z, y)
 \end{aligned}$$

$$\begin{aligned}
 \text{self-energy} &= \frac{\lambda}{2} G_F(x, x) & \text{red circle} &= -\frac{\lambda^2}{6} G_F(x, z)^3 & \text{green circle} &= -\frac{\lambda^2}{6} G_\rho(x, z)^3 \\
 \text{red circle} &= -\frac{\lambda^2}{6} G_F(x, z) G_\rho(x, z)^2 & \text{green circle} &= -\frac{\lambda^2}{6} G_F(x, z)^2 G_\rho(x, z)
 \end{aligned}$$

Relativistic Kadanoff-Baym equations

Homogeneous system

$$G(x, y) = G(x^0, y^0, \mathbf{x} - \mathbf{y}) \rightarrow G(x^0, y^0, \mathbf{k}), \quad \mathbf{k} = (k_x, k_y, k_z)$$

$$\left(\partial_{x^0}^2 + \mathbf{k}^2 + m^2 + \text{loop} \right) G_F(x^0, y^0, \mathbf{k}) =$$

$$\int_0^{y^0} dz^0 \left(\text{red circle} + \text{green circle} \right) G_\rho(z^0, y^0, \mathbf{k})$$

$$- \int_0^{x^0} dz^0 \left(\text{red circle} + \text{green circle} \right) G_F(z^0, y^0, \mathbf{k})$$

$$\text{loop} = \frac{\lambda}{2} \int \frac{d^3 p}{(2\pi)^3} G_F(x^0, x^0, \mathbf{p})$$

$$\text{red circle} = -\frac{\lambda^2}{6} \int \frac{d^3 p}{(2\pi)^3} \int \frac{d^3 q}{(2\pi)^3} G_F(x^0, z^0, \mathbf{p}) G_F(x^0, z^0, \mathbf{q}) G_F(x^0, z^0, \mathbf{k} - \mathbf{p} - \mathbf{q})$$

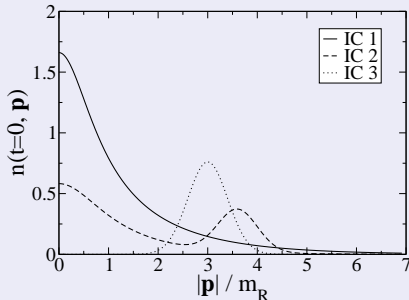
$$= -\frac{\lambda^2}{6} \int d^3 x e^{i\mathbf{k}\mathbf{x}} \left[\int \frac{d^3 p}{(2\pi)^3} e^{-i\mathbf{p}\mathbf{x}} G_F(x^0, z^0, \mathbf{p}) \right]^3 \quad \text{Danielewicz, Köhler, ...}$$

Relativistic Kadanoff-Baym equations

Initial conditions (Gaussian initial state)

Example: $\phi = \dot{\phi} = 0$,

$$\begin{aligned}G(x^0, y^0, \mathbf{p})|_{x^0=y^0=t_{init}} &= \frac{n_{\mathbf{p}}(t_{init}) + 1/2}{\omega_{\mathbf{p}}(t_{init})} \\(\partial_{x^0} + \partial_{y^0})G(x^0, y^0, \mathbf{p})|_{x^0=y^0=t_{init}} &= 0 \\ \partial_{x^0}\partial_{y^0}G(x^0, y^0, \mathbf{p})|_{x^0=y^0=t_{init}} &= \omega_{\mathbf{p}}(t_{init})(n_{\mathbf{p}}(t_{init}) + 1/2)\end{aligned}$$



$$\omega_{\mathbf{p}}(t_{init}) = \sqrt{m_R^2 + \mathbf{k}^2}$$

NR nuclear coll: *Danielewicz (1983); Köhler (1994,...); ...*

- Thermalization in relativistic scalar QFT

Berges, Cox (2001); Berges (2002); Aarts, Berges (2002); Aarts, Resco (2003); Juchem, Cassing, Greiner (2004); Arrizabalaga, Smit, Tranberg (2005); Lindner, Müller (2006); Gasenzer, Pawłowski (2008); ...

- Thermalization in relativistic fermionic QFT

Berges, Borsanyi, Serreau (2003); Lindner, Müller (2008)

- Prethermalization

Berges, Borsanyi, Wetterich (2004)

- Nonequilibrium Instabilities, Parametric Resonance

Berges, Serreau (2003), Aarts, Tranberg (2007); Berges, Rothkopf, Schmidt (2008); Berges, Pruschke, Rothkopf (2009)

- 2PI renormalization *Borsanyi,Reinosa (2008); MG, Müller (2009)*

Leptogenesis/Baryogenesis [no two-time KBE analysis yet]

Buchmüller, Fredenhagen (2000); DeSimone, Riotto (2007); Anisimov, Buchmüller, Drewes, Mendizabal (2008,10); MG, Hohenegger, Kartavtsev, Lindner (2009,10); Gagnon (2009)

NR nuclear coll: Danielewicz (1983); Köhler (1994,...); ...

- Thermalization in relativistic scalar QFT

Berges, Cox (2001); Berges (2002); Aarts, Berges (2002); Aarts, Resco (2003); Juchem, Cassing, Greiner (2004); Arrizabalaga, Smit, Tranberg (2005); Lindner, Müller (2006); Gasenzer, Pawłowski (2008); ...

- Thermalization in relativistic fermionic QFT

Berges, Borsanyi, Serreau (2003); Lindner, Müller (2008)

- Prethermalization

Berges, Borsanyi, Wetterich (2004)

- Nonequilibrium Instabilities, Parametric Resonance

Berges, Serreau (2003), Aarts, Tranberg (2007); Berges, Rothkopf, Schmidt (2008); Berges, Pruschke, Rothkopf (2009)

- **2PI renormalization** *Borsanyi,Reinosa (2008); MG, Müller (2009)*

Leptogenesis/Baryogenesis [no two-time KBE analysis yet]

Buchmüller, Fredenhagen (2000); DeSimone, Riotto (2007); Anisimov, Buchmüller, Drewes, Mendizabal (2008,10); MG, Hohenegger, Kartavtsev, Lindner (2009,10); Gagnon (2009)

UV Divergences

$$\begin{aligned} \text{---} \circ \text{---} &= \frac{\lambda}{2} \int \frac{d^3 p}{(2\pi)^3} G_{F,0}(x^0, x^0, p) \\ &= \frac{\lambda}{2} \int \frac{d^3 p}{(2\pi)^3} \frac{n_p + \frac{1}{2}}{\sqrt{m^2 + \mathbf{p}^2}} \sim \Lambda^2 \end{aligned}$$

$$\int dz^0 \text{---} \circ \text{---} G(z^0, y^0, k) \sim \Lambda^2$$

UV cut-off $|\mathbf{p}| \leq k_{max} \equiv \Lambda \quad \Rightarrow \quad \text{Quadratic divergence}$

Problem

- Gaussian initial states
- 'bare' particles in the initial state
- Incompatible with renormalization

Why does the Gaussian initial state lead to singularities ?

$$E_{total} = E_{kin}(t) + E_{corr}(t)$$

$$E_{kin}(t) = \frac{1}{2} \int \frac{d^3 k}{(2\pi)^3} \left[\partial_{x^0} \partial_{y^0} + \mathbf{k}^2 + m_R^2 + \text{---} \otimes \text{---} \right. \\ \left. + \text{---} \bullet \text{---} + \text{---} \otimes \text{---} \right] \text{---} \bullet |_{x^0=y^0=t} + \delta\Lambda$$

$\delta m^2, \delta Z$

$\delta\lambda$

$$E_{corr}(t) = \int_0^t dz^0 \int \frac{d^3 k}{(2\pi)^3} \text{---} \bullet \text{---} \bullet \text{---} \bullet |_{x^0=y^0=t}$$

- $E_{corr}(t)$ contains divergences
- $E_{kin}(t)$ contains 2PI counterterms

Berges, Borsanyi, Reinosa, Serreau (2004, 2005)

Why does the Gaussian initial state lead to singularities ?

$$E_{total} = E_{kin}(t) + E_{corr}(t)$$

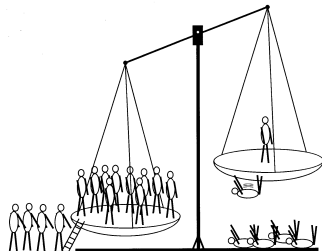
$$E_{kin}(t) = \frac{1}{2} \int \frac{d^3k}{(2\pi)^3} \left[\partial_{x^0} \partial_{y^0} + \mathbf{k}^2 + m_R^2 + \text{---} \otimes \text{---} \right. \\ \left. + \text{---} \circ \text{---} + \text{---} \otimes \text{---} \right] \text{---} \bullet |_{x^0=y^0=t} + \delta\Lambda$$

$\delta m^2, \delta Z$

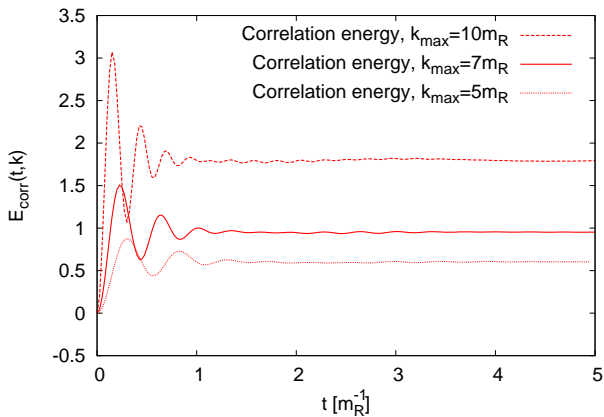
$\delta\lambda$

$$E_{corr}(t) = \int_0^t dz^0 \int \frac{d^3k}{(2\pi)^3} \text{---} \bullet \text{---} \circ \text{---} \bullet |_{x^0=y^0=t}$$

- $E_{corr}(t)$ contains divergences
- $E_{kin}(t)$ contains 2PI counterterms
Berges, Borsanyi, Reinosa, Serreau (2004, 2005)
- $E_{corr}(t)|_{t=0} = 0$ for Gaussian initial state
- \Rightarrow unbalanced divergence at $t = 0$



Why does the Gaussian initial state lead to singularities ?



Non-Gaussian initial state

- *Explicit:* non-Gaussian density matrix ρ at $t = t_{init}$
 - imaginary time-stepping $\rho = \exp(-\mathcal{O})$
 - initial n -point correlation functions

$$\langle \varphi_+ | \rho | \varphi_- \rangle = \exp \left(i \sum_{n=0}^{\infty} \int_{x_i} \alpha_n^{\epsilon_1 \dots \epsilon_n}(\mathbf{x}_1, \dots, \mathbf{x}_n) \varphi_{\epsilon_1}(\mathbf{x}_1) \cdots \varphi_{\epsilon_n}(\mathbf{x}_n) \right)$$

$$\text{where } \Phi(t_{init}, \mathbf{x}) | \varphi_{\pm} \rangle = \varphi_{\pm}(\mathbf{x}) | \varphi_{\pm} \rangle \quad [\text{Calzetta, Hu}]$$

e.g. Hall, Kukharev, Tikhodeev, Danielewicz, Wagner, Schlages, Bornath, Semkat, Kremp, Bonitz, Köhler, Morozov, Röpke,...

- *Implicit*
 - external two-point source $K(x, y)$ for $t < t_{init}$
e.g. Borsanyi, Reinosa,...

Gaussian initial state

All n -point correlation functions vanish at $t = t_{init}$ for $n \geq 3$

$$\alpha_n(x_1, \dots, x_n) = 0 \quad \text{for } n \geq 3$$

Renormalized initial state

Relevant n -point correlation functions asymptotically agree with vacuum correlations at short distances [for $n \leq 4$]

$$\alpha_n(x_1, \dots, x_n) = \alpha_n^{vac/th}(x_1, \dots, x_n) + \Delta\alpha_n(x_1, \dots, x_n)$$

Initial n -point correlation functions:

Local standard vertices:

$$\begin{array}{c} \diagup \\ \bullet \\ \diagdown \end{array} = -i\lambda_R, \quad \begin{array}{c} \diagup \\ \otimes \\ \diagdown \end{array} = -i\delta\lambda$$

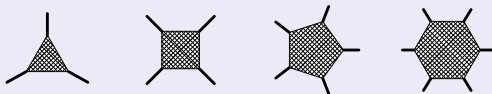
UV divergences, renormalization and non-Gaussian ICs

Initial n -point correlation functions:

Local standard vertices:

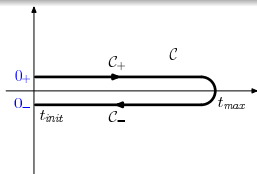
$$\begin{array}{c} \diagup \\ \bullet \\ \diagdown \end{array} = -i\lambda_R, \quad \begin{array}{c} \diagup \\ \otimes \\ \diagdown \end{array} = -i\delta\lambda$$

Effective non-local vertices: $\alpha_n(\mathbf{x}_1, \dots, \mathbf{x}_n)$



... encode the non-Gaussian initial correlations

$$\alpha_n(\mathbf{x}_1, \dots, \mathbf{x}_n) = \sum_{\epsilon_i \in \pm} \alpha_n^{\epsilon_1, \dots, \epsilon_n}(\mathbf{x}_1, \dots, \mathbf{x}_n) \times \delta(x_1^0 - 0_{\epsilon_1}) \cdots \delta(x_n^0 - 0_{\epsilon_n})$$



$$\alpha_n^{\epsilon_1, \dots, \epsilon_n}(\mathbf{x}_1, \dots, \mathbf{x}_n), \quad \epsilon_i \in \{+, -\} \Leftrightarrow \text{IC for } (\partial_{x_1^0})^{\epsilon_1} \cdots (\partial_{x_n^0})^{\epsilon_n} V_n(\mathbf{x}_1, \dots, \mathbf{x}_n), \quad c_i \in \{0, 1\}$$

Example: Initial 4-point correlation, 2PI three-loop truncation

$$\begin{aligned}
 \Gamma_2[G, \alpha_4] &= \text{Diagram 1} + \text{Diagram 2} + \text{Diagram 3} + \text{Diagram 4} + \text{Diagram 5} \\
 \Pi[G, \alpha_4] &= \underbrace{\text{Diagram 6} + \text{Diagram 7}}_{\Pi_{Gauss}} + \underbrace{\text{Diagram 8} + \text{Diagram 9}}_{\Pi_{\lambda\alpha}} + \underbrace{\text{Diagram 10} + \text{Diagram 11}}_{\Pi_{\alpha\lambda}} + \underbrace{\text{Diagram 12} + \text{Diagram 13}}_{\Pi_{\alpha\alpha}}
 \end{aligned}$$

The diagrams represent various Feynman diagrams for the 2PI three-loop truncation. The first row shows the two-particle irreducible (2PI) diagrams, and the second row shows the self-energy diagrams. The diagrams are grouped into four categories: Π_{Gauss} (Gaussian), $\Pi_{\lambda\alpha}$, $\Pi_{\alpha\lambda}$, and $\Pi_{\alpha\alpha}$ (non-Gaussian).

UV divergences, renormalization and non-Gaussian ICs

Example: Initial 4-point correlation, 2PI three-loop truncation

$$\Gamma_2[G, \alpha_4] = \text{diagram 1} + \text{diagram 2} + \text{diagram 3} + \text{diagram 4} + \text{diagram 5}$$

$$\Pi[G, \alpha_4] = \underbrace{\text{diagram 6} + \text{diagram 7}}_{\Pi_{Gauss}} + \underbrace{\text{diagram 8} + \text{diagram 9}}_{\Pi_{\lambda\alpha}} + \underbrace{\text{diagram 10} + \text{diagram 11}}_{\Pi_{\alpha\lambda}} + \underbrace{\text{diagram 12} + \text{diagram 13}}_{\Pi_{\alpha\alpha}}$$

Initial-time surface contribution

e.g. Danielewicz, Semkat, Kremp, Bonitz, ...

For the example:

$$\Pi_{\lambda\alpha}(x, z) = -\frac{\lambda}{6} \int_{\mathcal{C}} d^4 y_{123} G(x, y_1) G(x, y_2) G(x, y_3) \alpha_4(y_1, y_2, y_3, z)$$

In general:

$$\Pi_{\lambda\alpha}(x, z) = \Pi_{\lambda\alpha}^+(x, z) \delta(z^0 - 0_+) + \Pi_{\lambda\alpha}^-(x, z) \delta(z^0 - 0_-)$$

UV divergences, renormalization and non-Gaussian ICs

$$\left(\partial_{x^0}^2 + \mathbf{k}^2 + m_R^2 + \underbrace{\text{---}\otimes\text{---}}_{\delta m^2, \delta Z} + \text{---}\text{---}\text{---} + \underbrace{\text{---}\otimes\text{---}}_{\delta \lambda} \right) G_F(x, y) = \int_0^{y^0} d^4 z \text{---}\text{---}\text{---} G_\rho(z, y) - \int_0^{x^0} d^4 z \text{---}\text{---}\text{---} G_F(z, y) - \int_{\mathbf{c}} d^4 z \text{---}\text{---}\text{---} G(z, y)$$

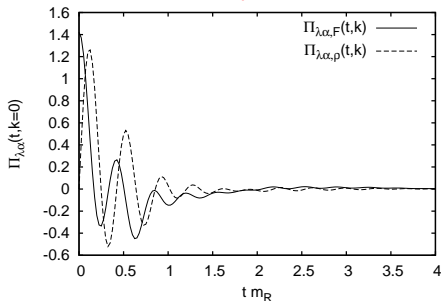
$\swarrow \delta(z^0 - t_{init})$

$$\left(\partial_{x^0}^2 + \mathbf{k}^2 + m_R^2 + \underbrace{\text{---}\otimes\text{---}}_{\delta m^2, \delta Z} + \text{---}\text{---}\text{---} + \underbrace{\text{---}\otimes\text{---}}_{\delta \lambda} \right) G_\rho(x, y) = \int_{x^0}^{y^0} d^4 z \text{---}\text{---}\text{---} G_\rho(z, y)$$

Non-Gaussian contribution on the right-hand side:

$$\int_{\mathbf{c}} d^4 z \Pi_{\lambda\alpha}(x, z) G(z, y) = \int d^3 z \Pi_{\lambda\alpha}(x, z) G(z^0 = 0, z, y)$$

e.g. Danielewicz, Semkat, Kremp, Bonitz, ...



UV divergences, renormalization and non-Gaussian ICs

Correlation energy at initial time

$$E_{kin}(t=0) = \frac{1}{2} \left[\partial_{x^0} \partial_{y^0} + \nabla^2 + m_R^2 + \underbrace{\text{---} \otimes \text{---}}_{\delta m^2, \delta Z} + \text{---} \circlearrowleft + \underbrace{\text{---} \otimes \text{---}}_{\delta \lambda} \right] \text{---} \bullet \Big|_{x=0} + \delta \Lambda$$

$$E_{corr}^{4-p.}(t=0) = \frac{i}{4} \int_{\mathcal{C}} d^4 z [\Pi_{Gauss}(x, z) + \Pi_{non-Gauss}(x, z)] G(z, x) \Big|_{x=0}$$

$$= \underbrace{\int_0^t dz^0 \text{---} \circlearrowleft \text{---} \bullet \Big|_{x=0}}_{\rightarrow 0} + \text{---} \circlearrowleft \text{---} \text{---} \text{---} \bullet \Big|_{x=0}$$

$$= \text{---} \circlearrowleft \text{---} \text{---} \text{---} \bullet \Big|_{x=0}$$

UV divergences, renormalization and non-Gaussian ICs

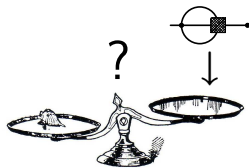
Correlation energy at initial time

$$E_{kin}(t=0) = \frac{1}{2} \left[\partial_{x^0} \partial_{y^0} + \nabla^2 + m_R^2 + \underbrace{\text{---} \otimes \text{---}}_{\delta m^2, \delta Z} + \text{---} \circlearrowleft \text{---} + \underbrace{\text{---} \otimes \text{---}}_{\delta \lambda} \right] \text{---} \bullet \Big|_{x=0} + \delta \Lambda$$

$$E_{corr}^{4-p.}(t=0) = \frac{i}{4} \int \frac{d^4 z}{c} [\Pi_{Gauss}(x, z) + \Pi_{non-Gauss}(x, z)] G(z, x) \Big|_{x=0}$$

$$= \underbrace{\int_0^t dz^0 \text{---} \bullet \text{---} \circlearrowleft \text{---} \bullet \text{---} \Big|_{x=0}}_{\rightarrow 0} + \text{---} \bullet \text{---} \circlearrowleft \text{---} \text{---} \Big|_{x=0}$$

$$= \text{---} \bullet \text{---} \circlearrowleft \text{---} \text{---} \Big|_{x=0}$$



Questions

- Is it sufficient to include α_4 , or does one need α_6 etc. ?
- How to choose α_n ?

Renormalized initial state

$$\alpha_n(x_1, \dots, x_n) = \alpha_n^{\text{vac/th}}(x_1, \dots, x_n) + \Delta\alpha_n(x_1, \dots, x_n)$$

UV divergences, renormalization and non-Gaussian ICs

Full **renormalized** thermal correlation energy (computed at initial time):

$$\begin{aligned}
 E_{corr}^{eq}(t=0) &= \frac{i}{4} \int \frac{d^4 z}{c} [\Pi_{Gauss}(x, z) + \Pi_{non-Gauss}(x, z)] G(z, x) \Big|_{x=0} \\
 &= \underbrace{\text{Diagram 1}}_{\int_0^{x^0} dz^0 \rightarrow 0} + \underbrace{\text{Diagram 2}}_{\int_0^{x^0} dz^0 \rightarrow 0} + \underbrace{\text{Diagram 3}}_{\int_0^{x^0} dz^0 \rightarrow 0} \\
 &+ \underbrace{\text{Diagram 4}}_{\int_0^{x^0} dz^0 \rightarrow 0} + \underbrace{\text{Diagram 5}}_{\int_0^{x^0} dz^0 \rightarrow 0} + \underbrace{\text{Diagram 6}}_{\int_0^{x^0} dz^0 \rightarrow 0} + \dots
 \end{aligned}$$

The diagrams represent Feynman diagrams for the thermal correlation energy. Each diagram consists of a horizontal line with a red dot on the left and a black dot on the right. A vertical line is attached to the red dot, and a circle is attached to the black dot. The diagrams are arranged in two rows. The first row contains three diagrams, and the second row contains three diagrams followed by an ellipsis. Each diagram is enclosed in a blue box. Below each diagram is a bracket and the text $\int_0^{x^0} dz^0 \rightarrow 0$.

UV divergences, renormalization and non-Gaussian ICs

Full **renormalized** thermal correlation energy (computed at initial time):

$$\begin{aligned}
 E_{corr}^{eq}(t=0) &= \frac{i}{4} \int \frac{d^4 z}{c} [\Pi_{Gauss}(x, z) + \Pi_{non-Gauss}(x, z)] G(z, x) \Big|_{x=0} \\
 &= \underbrace{\text{Diagram 1}}_{\int_0^{x^0} dz^0 \rightarrow 0} + \underbrace{\text{Diagram 2}}_{\int_0^{x^0} dz^0 \rightarrow 0} + \underbrace{\text{Diagram 3}}_{\int_0^{x^0} dz^0 \rightarrow 0} \\
 &\quad + \underbrace{\text{Diagram 4}}_{\int_0^{x^0} dz^0 \rightarrow 0} + \underbrace{\text{Diagram 5}}_{\int_0^{x^0} dz^0 \rightarrow 0} + \underbrace{\text{Diagram 6}}_{\int_0^{x^0} dz^0 \rightarrow 0} + \dots \\
 &= \text{Diagram 2} \Big|_{x=0} = E_{4-p, corr}^{eq}(t=0)
 \end{aligned}$$

The diagrams represent Feynman diagrams for the thermal correlation energy. Each diagram shows a horizontal line with a red dot at the right end, representing the initial time $x=0$. The diagrams are:

- Diagram 1: A circle with a red dot on the right side.
- Diagram 2: A circle with a red dot on the right side and a blue square box around it.
- Diagram 3: A circle with a red dot on the right side and a blue square box around it, with a smaller circle inside the box.
- Diagram 4: A circle with a red dot on the right side and a blue square box around it, with two smaller circles inside the box.
- Diagram 5: A circle with a red dot on the right side and a blue square box around it, with four smaller circles inside the box.
- Diagram 6: A circle with a red dot on the right side and a blue square box around it, with eight smaller circles inside the box.

 Below each diagram is a bracket and the text $\int_0^{x^0} dz^0 \rightarrow 0$, indicating that the contribution of each diagram vanishes as the initial time x^0 goes to zero.

...only the thermal **4-point** correlation contributes
 \Rightarrow truncate initial correlations with $n > 4$

Gaussian IC

$$G(x, y)|_{x^0, y^0=0} = G_{th}(x, y)|_{x^0, y^0=0}$$

$$\alpha_4(x_1, \dots, x_4) = 0$$

$$\alpha_n(x_1, \dots, x_n) = 0 \quad \text{for } n > 4$$

Non-Gaussian IC with α_4^{th}

$$G(x, y)|_{x^0, y^0=0} = G_{th}(x, y)|_{x^0, y^0=0}$$

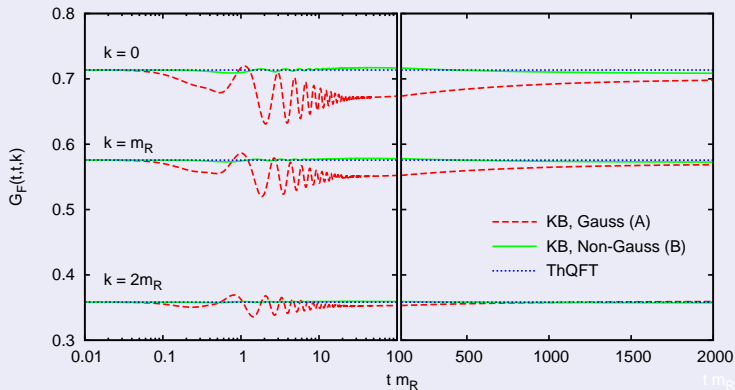
$$\alpha_4(x_1, \dots, x_4) = \alpha_4^{th}(x_1, \dots, x_4)$$

$$\alpha_n(x_1, \dots, x_n) = 0 \quad \text{for } n > 4$$

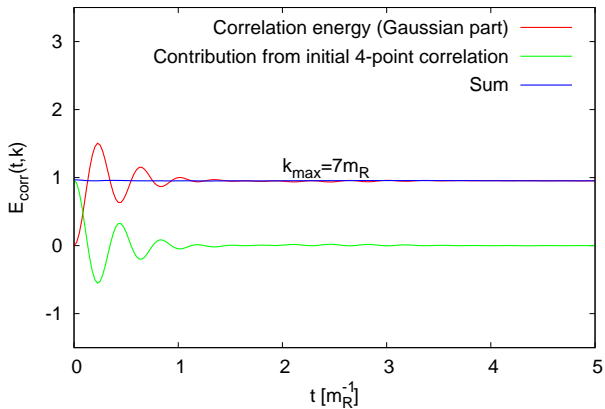
- Truncate thermal initial correlations
- \Rightarrow *nonequilibrium* initial states
- The upper states are 'as thermal as possible'
- Expectation: Non-Gaussian state more close to equilibrium

Minimal offset from thermal equilibrium

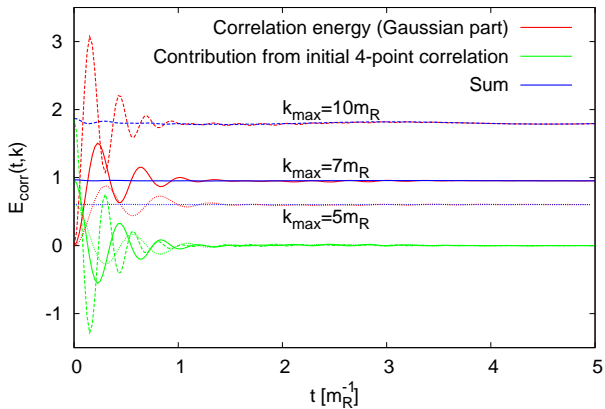
MG, Müller (2009)



Results for $\lambda\Phi^4$ 3-loop



Results for $\lambda\Phi^4$ 3-loop



Gaussian IC

$$\begin{aligned} E_{total} &= E_{kin}^{eq}(T_{init}) \\ &= E_{kin}^{eq}(T_{final}) + E_{corr}^{eq}(T_{final}) \end{aligned}$$

\Rightarrow e.g. Köhler, Morawetz, ...

$$T_{init} \neq T_{final}$$

Cutoff-divergence $E_{corr}^{eq} \sim \Lambda^4 + T^2\Lambda^2 + \dots$

$$|T_{init} - T_{final}| \sim \Lambda^2$$



Results for $\lambda\Phi^4$ 3-loop

Gaussian IC

$$\begin{aligned} E_{total} &= E_{kin}^{eq}(T_{init}) \\ &= E_{kin}^{eq}(T_{final}) + E_{corr}^{eq}(T_{final}) \end{aligned}$$

\Rightarrow e.g. Köhler, Morawetz, ...

$$T_{init} \neq T_{final}$$

Cutoff-divergence $E_{corr}^{eq} \sim \Lambda^4 + T^2\Lambda^2 + \dots$

$$|T_{init} - T_{final}| \sim \Lambda^2$$



Non-Gaussian IC with α_4^{th}

$$\begin{aligned} E_{total} &= E_{kin}^{eq}(T_{init}) + E_{4-p. corr}^{eq}(T_{init}) \\ &= E_{kin}^{eq}(T_{final}) + E_{corr}^{eq}(T_{final}) \end{aligned}$$

$$E_{4-p. corr}^{eq} = \text{diagram} = E_{corr}^{eq} \Rightarrow$$

$$T_{init} = T_{final}$$

No Cutoff-divergence

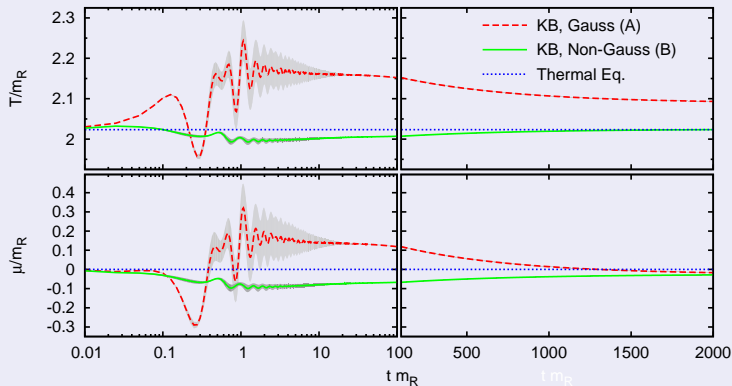
$$E_{total} = E^{eq}(T_{init}) = E^{eq}(T_{final}) = \text{finite}$$



Results for $\lambda\Phi^4$ 3-loop

No offset between initial and final temperature

MG, Müller (2009)



Renormalization of relativistic KBEs: status

MG, Müller (2009)

- It is necessary to include initial 4-point correlation α_4

$$\Gamma_2[G, \alpha_4] = \text{diagram 1} + \text{diagram 2} + \text{diagram 3} + \text{diagram 4} + \text{diagram 5}$$

- Choosing $\alpha_4 = \alpha_4^{2PI, vac/th}$ renormalizes total (initial) energy

$$\text{shaded square} = \text{blue square with diagonal lines}$$

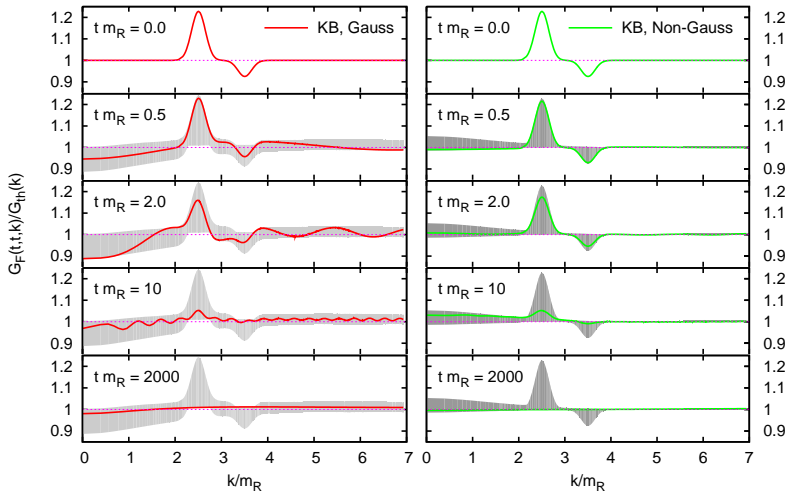
Restriction: Special class of ICs (close to equilibrium); $t \rightarrow 0, \infty$

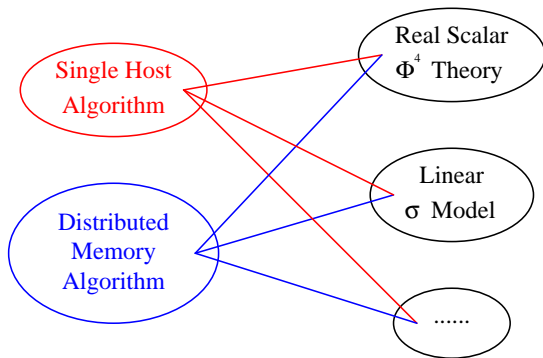
Questions

General conditions for renormalized initial states

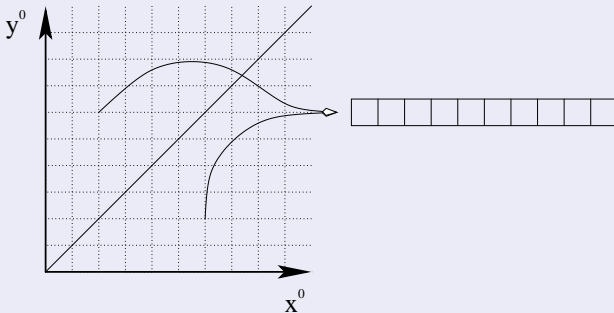
Results for $\lambda\Phi^4$ 3-loop

Example: $G(x^0, y^0, \mathbf{k})|_{x^0=y^0=t_{init}} = G_{vac/th}^{2PI}(\mathbf{k}) + \underbrace{\Delta G(\mathbf{k})}_{\rightarrow 0 \text{ for } k \rightarrow \infty}$, $\alpha_4 \in \{0, \alpha_4^{2PI, vac/th}\}$

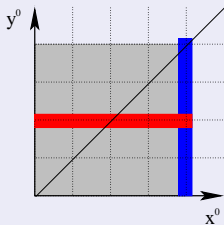




Single host algorithm: memory layout



Computation of self-energies and memory integrals



- Self-energy vector for $0 \leq y^0 \leq x^0$ using Fourier trf.

e.g. Danielewicz, Köhler, ...

$$\Pi(x^0, y^0, \hat{\mathbf{k}}) = -\frac{\lambda^2}{6} \sum_{\hat{\mathbf{x}}} e^{i\hat{\mathbf{k}}\hat{\mathbf{x}}} \left[\sum_{\hat{\mathbf{p}}} e^{-i\hat{\mathbf{p}}\hat{\mathbf{x}}} G(x^0, y^0, \hat{\mathbf{p}}) \right]^3$$

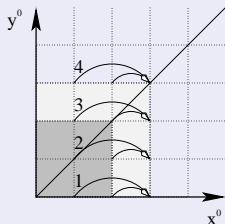
- Memory integrals = **history matrix** \times **self-energies**

$$MEMINT(x^0, y^0, \hat{\mathbf{k}}) = \sum_{z^0} \Pi(x^0, z^0, \hat{\mathbf{k}}) G(z^0, y^0, \hat{\mathbf{k}})$$

time-stepping

$$\begin{aligned} \partial_{x^0}^2 G(x^0, y^0, k) &\rightarrow \Delta_0^b \Delta_0^f G(x^0, y^0, \hat{\mathbf{k}}) \\ &= \frac{G(x^0 + a_t, y^0, \hat{\mathbf{k}}) - 2G(x^0, y^0, \hat{\mathbf{k}}) + G(x^0 - a_t, y^0, \hat{\mathbf{k}})}{a_t^2} \end{aligned}$$

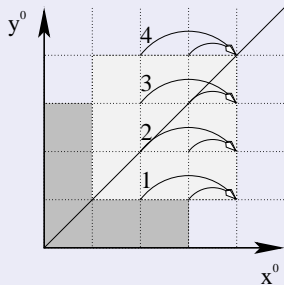
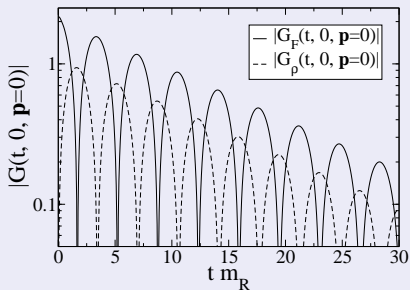
$$\begin{aligned} G(x^0 + a_t, y^0, \hat{\mathbf{k}}) &= 2G(x^0, y^0, \hat{\mathbf{k}}) - G(x^0 - a_t, y^0, \hat{\mathbf{k}}) \\ &\quad + a_t^2 \left[\text{MEMINT}(x^0, y^0, \hat{\mathbf{k}}) - (\hat{\mathbf{k}}^2 + M^2(x^0)) G(x^0, y^0, \hat{\mathbf{k}}) \right] \end{aligned}$$



Step 4: Use

$$\begin{aligned} G_F(x^0, y^0, \hat{\mathbf{k}}) &= G_F(y^0, x^0, \hat{\mathbf{k}}) \\ G_\rho(x^0, y^0, \hat{\mathbf{k}}) &= -G_\rho(y^0, x^0, \hat{\mathbf{k}}) \end{aligned}$$

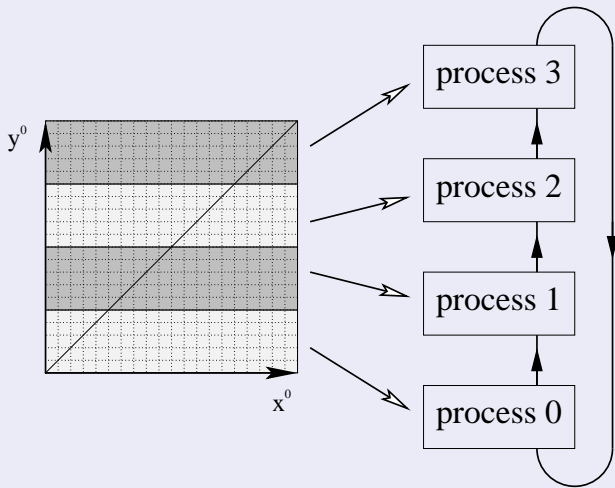
History cut-off



$$H = \{0, a_t, 2a_t, \dots, (N_t - 1) a_t\}^2$$

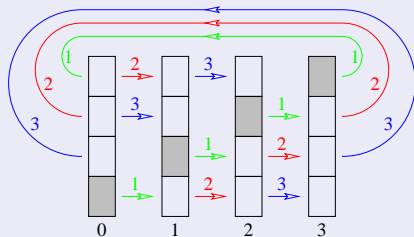
$$G(x^0, y^0, \hat{\mathbf{k}}) \rightarrow G(x^0 \bmod N_t, y^0 \bmod N_t, \hat{\mathbf{k}})$$

Parallelized distributed memory algorithm



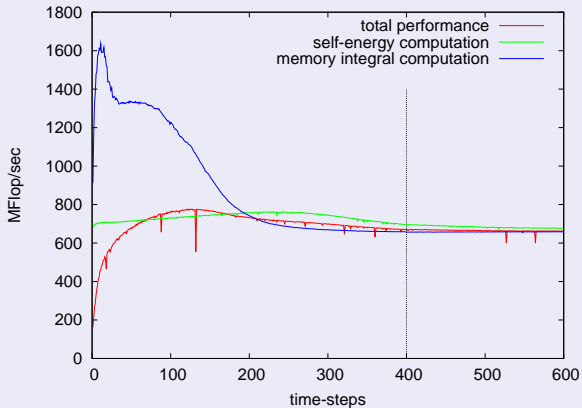
Parallelized distributed memory algorithm

- compute self-energies on each stripe in parallel
- circulate self-energies



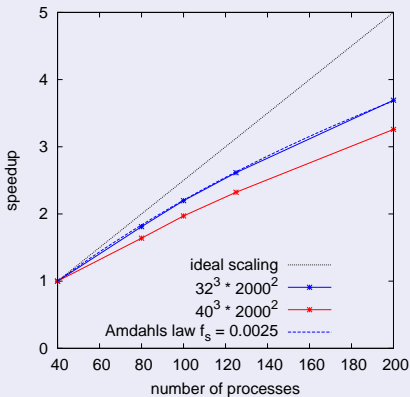
- compute memory integrals on each stripe in parallel
- time-stepping $(x^0, y^0) \rightarrow (x^0 + a_t, y^0)$ on each stripe in parallel
- mirror history matrix
- time-stepping $(x^0, x^0 + a_t) \rightarrow (x^0 + a_t, x^0 + a_t)$

Performance



Intel Itanium2 Montecito Dual Core 1.6GHz, Peak performance 6.4 GFlop/s per core

Scaling



$$s(N_p) = \frac{1}{f_s + \frac{f_p}{N_p} + k(N_p - 1)}$$

$$f_s : f_p \simeq 3 : 1000$$



LRZ, HLRB2 (SGI Altix 4700, 9728 cores, Total peak performance 62.3 TFlop/s)

Relativistic KBEs for correlated initial states and baryogenesis

thank you!



References

- MG, Markus Michael Müller, *Phys.Rev.D80:085011,2009*
- Borsanyi, Reinosu *Nucl.Phys.A820:147C,2009*
- MG, Markus Michael Müller, *proceedings of HLRB2 results workshop 2009*
- MG, Hohenegger, Kartavtsev, Lindner, *Phys.Rev.D80:125027,2009;*
arXiv:0911.4122; arXiv:1002.0331

Thermal Initial Correlations

Thermal density matrix of the interacting theory

$$\rho_{th} = \frac{1}{Z} e^{-\beta H}, \quad H = H_0 + H_{int}$$

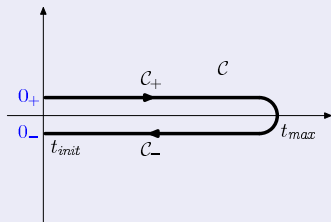
⇒ Compute the corresponding initial correlations

$$\langle \varphi_+ | \rho_{th} | \varphi_- \rangle = \exp \left(i \sum_{n=0}^{\infty} \int d^4 x_{12\dots n} \alpha_n^{th}(x_1, \dots, x_n) \varphi(x_1) \varphi(x_2) \cdots \varphi(x_n) \right)$$

- Can be done order-by-order in H_{int}
- Problem: Need approximations compatible with 2PI formalism
- Solution: Match 2PI on closed real-time path with 2PI thermal (imaginary-time) field theory *MG, Müller (2009)*

Thermal Initial Correlations

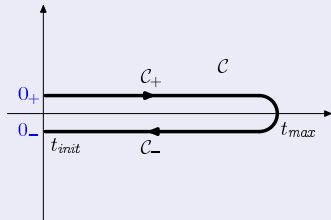
Closed time path \mathcal{C} with α_n



$$\begin{aligned} & \langle \varphi_+ | \rho_{th} | \varphi_- \rangle \\ &= \exp \left(i \sum_{n=0}^{\infty} \alpha_{12\dots n}^{th} \varphi_1 \varphi_2 \cdots \varphi_n \right) \end{aligned}$$

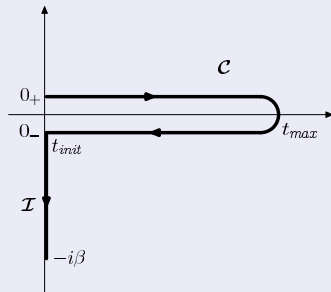
Thermal Initial Correlations

Closed time path \mathcal{C} with α_n



$$\begin{aligned} &\langle \varphi_+ | \rho_{th} | \varphi_- \rangle \\ &= \exp \left(i \sum_{n=0}^{\infty} \alpha_{12\dots n}^{th} \varphi_1 \varphi_2 \cdots \varphi_n \right) \end{aligned}$$

Thermal time path $\mathcal{C} + \mathcal{I}$



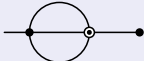
$$\begin{aligned} &\langle \varphi_+ | \rho_{th} | \varphi_- \rangle \\ &= \int_{\varphi(0,\mathbf{x})=\varphi_-(\mathbf{x})}^{\varphi(-i\beta,\mathbf{x})=\varphi_+(\mathbf{x})} \mathcal{D}\varphi \exp \left(i \int_{\mathcal{I}} d^4x \mathcal{L}(x) \right) \end{aligned}$$

Thermal Initial Correlations

Thermal time path $\mathcal{C} + \mathcal{I}$

Self-consistent Schwinger-Dyson equation

$$G_{th}^{-1}(x, y) = G_{0,th}^{-1}(x, y) - \Pi_{th}(x, y) \quad \Leftrightarrow$$

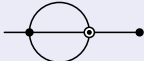
$$(\square_x + m^2)G_{th}(x, y) = -i\delta_{\mathcal{C}+\mathcal{I}}(x - y) - i \underbrace{\int_{\mathcal{C}+\mathcal{I}} d^4z \Pi_{th}(x, z) G_{th}(z, y)}_{\text{Diagram}}$$


Thermal Initial Correlations

Thermal time path $\mathcal{C} + \mathcal{I}$

Self-consistent Schwinger-Dyson equation

$$G_{th}^{-1}(x, y) = G_{0,th}^{-1}(x, y) - \Pi_{th}(x, y) \quad \Leftrightarrow$$

$$(\square_x + m^2)G_{th}(x, y) = -i\delta_{\mathcal{C}+\mathcal{I}}(x - y) - i \underbrace{\int_{\mathcal{C}+\mathcal{I}} d^4z \Pi_{th}(x, z) G_{th}(z, y)}_{\text{Diagram}}$$


Closed time path \mathcal{C} with initial correlations α

Kadanoff-Baym equation for a Non-Gaussian initial state

$$(\square_x + m^2)G(x, y) = -i\delta_{\mathcal{C}}(x - y) - i \int_{\mathcal{C}} d^4z [\Pi_{Gauss}(x, z) + \Pi_{non-Gauss}(x, z)] G(z, y)$$

Thermal Initial Correlations

Thermal time path $\mathcal{C} + \mathcal{I}$

The lines represent the *complete* propagator

$$\begin{aligned} G_{th}^{\mathcal{C}\mathcal{C}}(x, y) &= \bullet \text{---} \bullet & G_{th}^{\mathcal{C}\mathcal{I}}(x, y) &= \bullet \text{---} \circ \\ G_{th}^{\mathcal{I}\mathcal{I}}(x, y) &= \circ \text{---} \circ & G_{th}^{\mathcal{I}\mathcal{C}}(x, y) &= \circ \text{---} \bullet \\ -i\lambda \int_{\mathcal{C}} d^4x &= \text{X}(\bullet) & -i\lambda \int_{\mathcal{I}} d^4x &= \text{X}(\circ) & -i\lambda \int_{\mathcal{C}+\mathcal{I}} d^4x &= \text{X}(\bullet/\circ) \end{aligned}$$

Example: 2PI three-loop truncation

Thermal Initial Correlations: Perturbation Theory

$$G_{0,th}^{\mathcal{IC}}(-i\tau, y^0, \mathbf{k}) = \int_c dt \Delta_0(-i\tau, t, \mathbf{k}) G_{0,th}^{\mathcal{CC}}(t, y^0, \mathbf{k})$$

Free 'connection'

$$\begin{aligned} \Delta_0(-i\tau, z^0, \mathbf{k}) &= \Delta_0^+(-i\tau, \mathbf{k}) \delta_{\mathcal{C}}(z^0 - 0_+) + \Delta_0^-(-i\tau, \mathbf{k}) \delta_{\mathcal{C}}(z^0 - 0_-) \\ &= \dots\dots\dots | \text{---} \end{aligned}$$

where

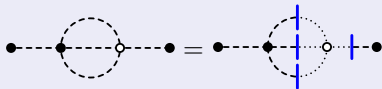
$$\Delta_0^+(-i\tau, \mathbf{k}) = \frac{\sinh(\omega_{\mathbf{k}}\tau)}{\sinh(\omega_{\mathbf{k}}\beta)} = \frac{G_{0,th}^{\mathcal{II}}(-i\tau, 0, \mathbf{k})}{2G_{0,th}(0, 0, \mathbf{k})} + \partial_{\tau} G_{0,th}^{\mathcal{II}}(-i\tau, 0, \mathbf{k})$$

$$\Delta_0^-(-i\tau, \mathbf{k}) = \frac{\sinh(\omega_{\mathbf{k}}(\beta - \tau))}{\sinh(\omega_{\mathbf{k}}\beta)} = \frac{G_{0,th}^{\mathcal{II}}(-i\tau, 0, \mathbf{k})}{2G_{0,th}(0, 0, \mathbf{k})} - \partial_{\tau} G_{0,th}^{\mathcal{II}}(-i\tau, 0, \mathbf{k})$$

Thermal Initial Correlations: Perturbation Theory

Example

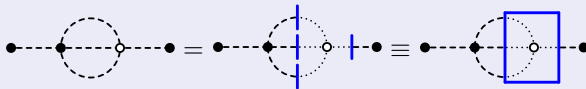
MG, Müller (2009)



Thermal Initial Correlations: Perturbation Theory

Example

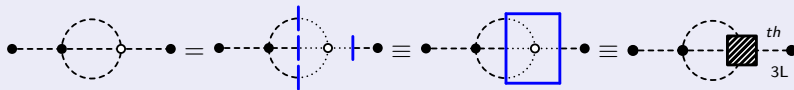
MG, Müller (2009)



Thermal Initial Correlations: Perturbation Theory

Example

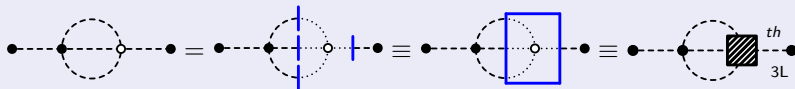
MG, Müller (2009)



Thermal Initial Correlations: Perturbation Theory

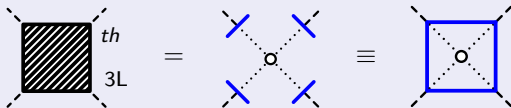
Example

MG, Müller (2009)



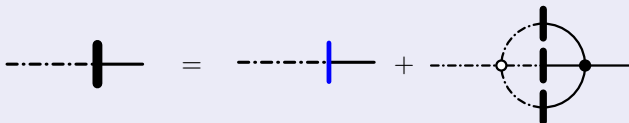
Perturbative initial 4-point correlation

$$\alpha_{4,3L}^{th}(z_1, z_2, z_3, z_4) = -i\lambda \int_{\mathcal{I}} d^4v \Delta_0(v, z_1) \Delta_0(v, z_2) \Delta_0(v, z_3) \Delta_0(v, z_4)$$



Example: 2PI three-loop truncation

MG, Müller (2009)



Example: 2PI three-loop truncation

MG, Müller (2009)

A diagrammatic equation showing the truncation of a 2PI diagram. On the left, a dashed line with a thick black vertical bar. This is equal to a dashed line with a blue vertical bar, plus a diagram consisting of a dashed line with a white circle, a solid line with a black circle, and a loop with two thick black vertical bars.

Iterative Solution:

A diagrammatic equation showing the iterative solution. On the left, a dashed line with a thick black vertical bar. This is equal to a dashed line with a blue vertical bar, plus a diagram consisting of a dashed line with a white circle, a solid line with a black circle, and a loop with two blue vertical bars.

Example: 2PI three-loop truncation

MG, Müller (2009)

A diagrammatic equation showing the decomposition of a two-point function. On the left is a thick vertical black bar representing a self-energy insertion. This is equal to the sum of two terms: a thin vertical blue bar representing a self-energy insertion, and a diagram of a loop with a thick vertical black bar and a thin vertical blue bar, representing a two-loop self-energy correction.

Iterative Solution:

A diagrammatic equation showing the iterative solution of the two-point function. The left side is the same as the previous equation. The right side is the sum of two terms: a thin vertical blue bar, and a diagram of a loop with a thin vertical blue bar and a thick vertical black bar, representing a two-loop self-energy correction. Below this is a plus sign followed by a diagram of a loop with a thin vertical blue bar and a thick vertical black bar, representing a two-loop self-energy correction.

Thermal Initial Correlations: 2PI

Example: 2PI three-loop truncation

MG, Müller (2009)

A diagrammatic equation showing the decomposition of a thick vertical bar on a dashed line into a blue vertical bar on a solid line plus a three-loop diagram. The three-loop diagram consists of a dashed line with a white circle at its end, connected to a solid line with a black circle at its end, which is then connected to a dashed line with a white circle at its end, which is finally connected to a solid line with a black circle at its end. A vertical line passes through the center of the diagram, with a thick black bar on the left and a thin black bar on the right.

Iterative Solution:

An iterative solution diagram showing the expansion of the thick vertical bar on a dashed line. The first row shows the thick bar equal to a blue bar on a solid line plus a three-loop diagram with a blue vertical line. The second row shows the three-loop diagram from the first row expanded into two more terms: a diagram with two nested three-loop structures and a diagram with two overlapping three-loop structures, both featuring a blue vertical line.

Thermal Initial Correlations: 2PI

Example: 2PI three-loop truncation

MG, Müller (2009)

A diagrammatic equation showing the decomposition of a thick vertical bar on a dashed line into a blue vertical bar on a solid line plus a diagram with a dashed circle and a thick vertical bar.

$$\text{---} \overline{\text{---}} \text{---} = \text{---} \text{---} \text{---} + \text{---} \text{---} \text{---}$$

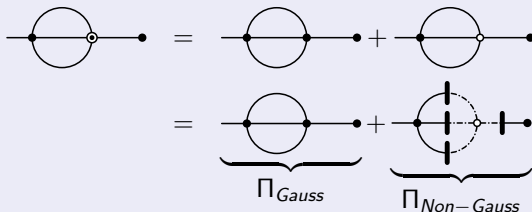
Iterative Solution:

A diagrammatic series representing the iterative solution. It starts with the thick vertical bar on a dashed line, followed by a plus sign and a blue vertical bar on a solid line, then a plus sign and a diagram with a dashed circle and a blue vertical bar. This is followed by three more terms, each with a plus sign and a diagram with a dashed circle and a blue vertical bar, showing increasing complexity with multiple loops. The series ends with a plus sign and an ellipsis.

$$\text{---} \overline{\text{---}} \text{---} = \text{---} \text{---} \text{---} + \text{---} \text{---} \text{---} + \text{---} \text{---} \text{---} + \text{---} \text{---} \text{---} + \text{---} \text{---} \text{---} + \dots$$

Example: 2PI three-loop truncation

MG, Müller (2009)



The diagram illustrates the 2PI three-loop truncation. It shows a sequence of equalities between Feynman diagrams. The first diagram is a circle with a horizontal line through its center, a solid dot on the left, and an open circle on the right. This is equal to the sum of two diagrams: one with a solid dot on the left and a solid dot on the right, and another with a solid dot on the left and an open circle on the right. The second equality shows the first diagram of the sum as a bracketed term labeled Π_{Gauss} , and the second diagram as a bracketed term labeled $\Pi_{Non-Gauss}$. The $\Pi_{Non-Gauss}$ diagram features a dashed circle with a vertical line through its center, a solid dot on the left, and a solid dot on the right.

$$\begin{aligned} \text{Diagram 1} &= \text{Diagram 2} + \text{Diagram 3} \\ &= \underbrace{\text{Diagram 2}}_{\Pi_{Gauss}} + \underbrace{\text{Diagram 3}}_{\Pi_{Non-Gauss}} \end{aligned}$$

Example: 2PI three-loop truncation

MG, Müller (2009)

$$\begin{aligned}
 \text{Diagram} &= \text{Diagram} + \text{Diagram} \\
 &= \underbrace{\text{Diagram}}_{\Pi_{Gauss}} + \underbrace{\text{Diagram}}_{\Pi_{Non-Gauss}}
 \end{aligned}$$

Non-Gaussian self-energy contains $\alpha_n^{th}(x_1, \dots, x_n)$ for all $n \geq 4$

$$\Pi_{non-Gauss}(x, z) = \text{Diagram}$$

Example: 2PI three-loop truncation

MG, Müller (2009)

$$\begin{aligned}
 \text{Diagram 1} &= \text{Diagram 2} + \text{Diagram 3} \\
 &= \underbrace{\text{Diagram 4}}_{\Pi_{Gauss}} + \underbrace{\text{Diagram 5}}_{\Pi_{Non-Gauss}}
 \end{aligned}$$

Non-Gaussian self-energy contains $\alpha_n^{th}(x_1, \dots, x_n)$ for all $n \geq 4$

$$\Pi_{non-Gauss}(x, z) = \text{Diagram 6} + \text{Diagram 7}$$

Example: 2PI three-loop truncation

MG, Müller (2009)

$$\begin{aligned}
 & \text{Diagram 1} = \text{Diagram 2} + \text{Diagram 3} \\
 & = \underbrace{\text{Diagram 4}}_{\Pi_{Gauss}} + \underbrace{\text{Diagram 5}}_{\Pi_{Non-Gauss}}
 \end{aligned}$$

Non-Gaussian self-energy contains $\alpha_n^{th}(x_1, \dots, x_n)$ for all $n \geq 4$

$$\Pi_{non-Gauss}(x, z) = \text{Diagram 1} + \text{Diagram 2} + \text{Diagram 3}$$

Example: 2PI three-loop truncation

MG, Müller (2009)

$$\begin{aligned}
 \text{Diagram} &= \text{Diagram}_1 + \text{Diagram}_2 \\
 &= \underbrace{\text{Diagram}_3}_{\Pi_{Gauss}} + \underbrace{\text{Diagram}_4}_{\Pi_{Non-Gauss}}
 \end{aligned}$$

Non-Gaussian self-energy contains $\alpha_n^{th}(x_1, \dots, x_n)$ for all $n \geq 4$

$$\Pi_{non-Gauss}(x, z) = \text{Diagram}_1 + \text{Diagram}_2 + \text{Diagram}_3 + \text{Diagram}_4$$

Example: 2PI three-loop truncation

MG, Müller (2009)

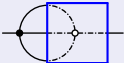
$$\begin{aligned}
 \text{Diagram 1} &= \text{Diagram 2} + \text{Diagram 3} \\
 &= \underbrace{\text{Diagram 4}}_{\Pi_{Gauss}} + \underbrace{\text{Diagram 5}}_{\Pi_{Non-Gauss}}
 \end{aligned}$$

Non-Gaussian self-energy contains $\alpha_n^{th}(x_1, \dots, x_n)$ for all $n \geq 4$

$$\begin{aligned}
 \Pi_{non-Gauss}(x, z) &= \text{Diagram 1} + \text{Diagram 2} + \text{Diagram 3} \\
 &+ \text{Diagram 4} + \text{Diagram 5} + \dots
 \end{aligned}$$

Result: Example for Setting-Sun Approximation

$$\Pi_{Gauss} = \text{---} \overset{\text{loop}}{\circlearrowleft} \text{---} + \text{---} \circ \text{---}$$

$$\Pi_{non-Gauss}^{th} = \text{---} \circ \text{---}$$


Result: Example for Setting-Sun Approximation

$$\Pi_{Gauss} = \text{---} \overset{\circlearrowleft}{\bullet} \text{---} + \text{---} \bullet \text{---} \circ \text{---} \bullet \text{---}$$

$$\Pi_{non-Gauss}^{th} = \text{---} \bullet \text{---} \circ \text{---} \bullet \text{---} + \text{---} \bullet \text{---} \circ \text{---} \bullet \text{---} \circ \text{---} \bullet \text{---}$$

Result: Example for Setting-Sun Approximation

$$\Pi_{Gauss} = \text{---} \overset{\circlearrowleft}{\bullet} \text{---} + \text{---} \bullet \text{---} \circ \text{---} \bullet \text{---}$$

$$\begin{aligned} \Pi_{non-Gauss}^{th} = & \text{---} \bullet \text{---} \circ \text{---} \bullet \text{---} + \text{---} \bullet \text{---} \circ \text{---} \bullet \text{---} \circ \text{---} \bullet \text{---} + \text{---} \bullet \text{---} \circ \text{---} \bullet \text{---} \circ \text{---} \bullet \text{---} \circ \text{---} \bullet \text{---} \\ & + \text{---} \bullet \text{---} \circ \text{---} \bullet \text{---} \circ \text{---} \bullet \text{---} \circ \text{---} \bullet \text{---} \end{aligned}$$

Result: Example for Setting-Sun Approximation

$$\Pi_{Gauss} = \text{---} \overset{\circlearrowleft}{\bullet} \text{---} + \text{---} \bullet \text{---} \bullet \text{---}$$

$$\begin{aligned} \Pi_{non-Gauss}^{th} = & \text{---} \bullet \text{---} \bullet \text{---} \text{---} \bullet \text{---} \bullet \text{---} + \text{---} \bullet \text{---} \bullet \text{---} \bullet \text{---} \bullet \text{---} \bullet \text{---} + \text{---} \bullet \text{---} \bullet \text{---} \bullet \text{---} \bullet \text{---} \bullet \text{---} \bullet \text{---} \\ & + \text{---} \bullet \text{---} \bullet \text{---} \bullet \text{---} \bullet \text{---} \bullet \text{---} \bullet \text{---} \bullet \text{---} + \text{---} \bullet \text{---} \bullet \text{---} \bullet \text{---} \bullet \text{---} \bullet \text{---} \bullet \text{---} \bullet \text{---} \bullet \text{---} + \dots \end{aligned}$$

UV divergences, renormalization and non-Gaussian ICs

Result: Example for Setting-Sun Approximation

$$\Pi_{Gauss} = \text{---} \overset{\circlearrowleft}{\circlearrowright} \text{---} + \text{---} \circ \text{---}$$
$$\Pi_{non-Gauss}^{th} = \text{---} \circ \text{---} + \text{---} \circ \text{---} \circ \text{---} + \text{---} \circ \text{---} \circ \text{---} \circ \text{---} + \dots$$

The diagrams for $\Pi_{non-Gauss}^{th}$ show a series of terms where the loop is enclosed in a blue box, representing a setting-sun approximation. The first row shows the first three terms, and the second row shows the next two terms followed by an ellipsis.

Kadanoff-Baym equations with thermal initial correlations contain

$$\alpha_n^{th}(x_1, \dots, x_n) \quad \text{for all } n \geq 4$$